



The primary energy spectrum estimation by using Linsley's EAS time structure with a compact air shower array

H. MATSUMOTO¹, A. IYONO¹, I. YAMAMOTO¹, K. OKEI², S. TSUJI², T. NAKATSUKA³,
N. OCHI⁴, S. OHARA⁵, T. KONISHI⁵, A. MUKAI⁵, M. SHIMADA⁵, N. TAKAHASHI⁶

¹Okayama University of Science, Okayama 700-0005, Japan

²Kawasaki Medical School, Kurashiki 701-0192, Japan

³Okayama Shoka University, Okayama 700-8601, Japan

⁴Yonago National College of Technology, Yonago 683-8502, Japan

⁵Nara Sangyo University, Nara 636-8503, Japan

⁶Hirosaki University, Hirosaki 036-8560, Japan

h_matsumoto@das.ous.ac.jp

DOI: 10.7529/ICRC2011/V01/0183

Abstract: The primary energy spectrum in the energy region of $10^{16} - 10^{19.5}$ eV has been studied by using a compact extensive air shower array and the Linsley's method. We obtained the power-law spectral indexes of $-2.54 (+0.22 - 0.24)$ and $-3.20 (+0.52 - 1.3)$ in the energy region of $10^{16} - 10^{19.5}$ eV and $10^{16} - 10^{18.5}$ eV, respectively. Additionally, in order to improve the energy resolution of the existing EAS array and suppress events leak in the energy spectrum from the low energy region to the high energy region, the apparatus for the event selection by restricting EAS zenith angle has been installed. The result of new observation are obtained that α are equal to $-3.13 (+0.22 - 0.24)$ and $-3.60 (+0.52 - 1.3)$ in the same energy region above, respectively.

Keywords: Energy spectrum, EAS time structure

1 Introduction

The investigation of the primary cosmic ray spectrum in the energy region above 10^{16} eV is important to understanding the acceleration mechanisms of cosmic rays. Various experiments as Auger [1], Yakutsk [2] and AGASA [3] have been performed, and such experiments have large observation array of which size are equal to several thousand km². As recent results of such experiments, the shape of primary spectra obtained by such experiments is consistent with each other while intensities are different.

We have estimated the primary cosmic ray energy and its spectrum by using a compact EAS array and the approach suggested by Linsley to estimate the primary energy from the EAS time structure, since April 2006. Recent studies have been reported on references [4, 5], and in this paper we present the primary energy spectrum obtained by using a new apparatus installed for improvement in the energy resolution.

2 Apparatus

The five compact EAS arrays are located at Okayama University of Science (OUS). These arrays are named OUS1, OUS2, OUS3, OUS4 and OUS5, and are maintained by

Large Area Air Shower (LAAS) group [7, 8, 9]. We use the OUS1 and the OUS4 in this analysis.

The OUS1 consists of eight plastic scintillation counters and is set as shown in Fig. 1-(a). Each detector is equipped with a scintillator (size 50cm \times 50cm \times 5cm) and a fast PMT, and is shielded with 5mm of stainless case. The detectors are installed on the rooftop of the building in the university campus and spread over an area of about 200m². The data acquisition system consists of a TDC, a ADC, and a shift register. When the system received the trigger request signal from a coincidence module, the observation data is acquired by each module. The trigger request signal is generated when more than three detector are hit within 2.5 μ s time window.

In order to observe the arrival time of EAS particles distributed up to several μ s, we use the shift register system. In the shift register system, the width of the time window to record EAS particle signals is 5 μ s, 0 second is set on when receiving the trigger request signal, and the signals can be recorded within $\pm 2.5\mu$ s time width. Each signal from detector is digitized with the shift register system with the time resolution of 5ns. The time stamp of triggered event is obtained by a GPS timing module and it provides the EAS arrival timing in Universal Time with 1 μ s accuracy.

The OUS4 shown in Fig 1-(b) and (c) is the apparatus for obtaining the EAS zenith angle information and is installed in the first floor of a four stories building which is located at about 10m distance from the OUS1. The OUS4 is set up two couple of the plastic scintillation counters (size 20cm × 50cm × 1cm) at top and bottom layer. And four sets of the same detector as the OUS1 are also installed. Those are used to eliminate EAS events with larger zenith angle than 25.6°. In the case of hitting only top and bottom detectors, and hitting top, bottom and side detectors, the EAS zenith angle information is determined within 25.6° and over 25.6°, respectively. The data acquisition system of the OUS4 is almost the same as the OUS1. EAS events are recorded by a TDC, a ADC, and a shift register system when both top and bottom detectors are hit within 2.5μs. The time stamp of EAS events are obtained by a GPS timing module, and the time information between the OUS1 and the OUS4 is synchronized within 1μs accuracy.

3 Estimation method and simulation

3.1 Core distance estimation

We apply the Linsley's method [10] to EAS core distance estimation. Linsley showed that the dispersion of arrival time distribution of EAS particles increase with the core distance r , the zenith angle θ and weakly depends on the primary energy E , and formulated this characteristic empirically. The dispersion σ_t is calculated by $\sigma_t = [\int (t - \langle t \rangle)^2 p(t) dt]^{1/2}$, where t is the arrival time of EAS particle and $p(t)$ is the probability density function of particles arriving in the differential time dt . The average behavior of dispersion $\langle \sigma_t \rangle$ can be described by the empirical formula

$$\langle \sigma_t \rangle = \sigma_{t0} \left(1 + \frac{r}{r_t} \right)^b, \quad (1)$$

where $\sigma_{t0} = 1.6$ ns, $r_t = 30$ m and $b = (2.08 \pm 0.08) - (0.4 \pm 0.06) \sec \theta + (0 \pm 0.06) \log(E/10^{17}\text{eV})$. Note that b value is used the \bar{b} value ($b \simeq \bar{b} = 1.65$) averaged by the EAS zenith angle distribution expected by our observation, and the contribution of E is ignored. We assume the probability density function $p(t)$ to be a gamma distribution as $p(t) = (t/\mu^2) \exp(-t/\mu)$, and then σ_t is obtained by $\sigma_t = \langle t \rangle^2/2$. However, we adopt the median t_{median} in the series of EAS particle arrival time as its estimator in this analysis [4]. σ_t is described as

$$\sigma_t = \frac{\sqrt{2}}{1.67} t_{\text{median}}. \quad (2)$$

r is calculated as Eq.3 by substituting Eq.2 into Eq.1 and rearranging Eq.1.

$$r = 30 \left((1.35 t_{\text{median}})^{(1/1.65)} \right). \quad (3)$$

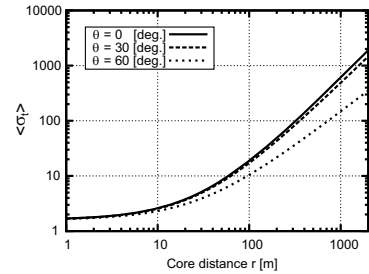


Figure 2: The dispersion $\langle \sigma_t \rangle$ as a function of r .

3.2 Primary energy estimation

The primary energy E is determined by using the lateral distribution of EAS particles obtained from detector simulations, and the EAS particles density ρ_{obs} and the core distance r_{obs} obtained from the OUS1 observation. The detector simulation was performed by using AIRES simulator [11]. The primary nuclei and hadronic interaction models were assumed to be protons and the QGSJETII-3 [12] and the Hillas Splitting Algorithm [13], respectively. The detail of the simulation procedure is shown in the reference [5].

The shift register system records the total number of EAS particles n obtained from the sum of the number of EAS particles in each detector, and arrival time t_i ($i = 1, 2, \dots, n$) of each EAS particle. ρ_{obs} is calculated by $\rho_{\text{obs}} = n/S$, where S is the total area of detector and $S = 2\text{m}^2$. Calculating the median value t_{median} from t_i , r_{obs} is obtained from substitute t_{median} for Eq.2. To estimate the EAS size from obtained ρ_{obs} and r_{obs} , we need the averaged lateral distribution $\bar{\rho}(r, E)$ integrated over the EAS zenith angle distribution which is expected by detector simulations. Finally, we can obtain E from comparing ρ_{obs} with $\bar{\rho}(r_{\text{obs}}, E)$.

3.3 Primary energy spectrum estimation

We assumed the primary energy spectrum to be the power law one $f(E) \propto E^\alpha$, where α is the spectral index and is sampled from -1.7 to -4.0 every 0.1 in the simulation. The obtained energy spectra $f'(E)$ are the convolution of $f(E)$ with energy resolution functions and the acceptance obtained by the detector simulation. The obtained $f'(E)$ is also described as $f'(E) \propto E^{\alpha'}$, where α' is the fitted spectral index. Actually, α' is obtained by data analysis and α is estimated by conversion from α' .

4 Data period and event selection criteria

The data period in the OUS1 observation used for this analysis is from April 2006 to December 2010, and the total observation time is 1366 days. The total number of events is 9.2×10^6 events and 9.1×10^4 events can be estimated those primary energy. In the synchronized observation be-

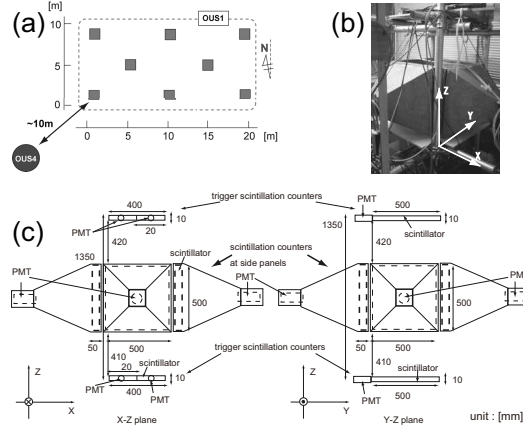


Figure 1: (a) The arrangement of the OUS1 and the OUS4. The square symbols represent detectors. (b) The OUS4 and (c) its X-Z and Y-Z views.

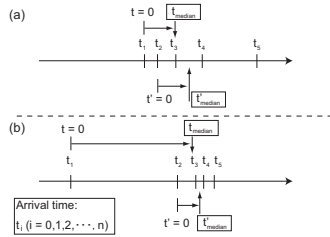


Figure 3: (a) In the case of $t'_\text{median}/t_\text{median} \geq 0.5$, we categorized all particles as coming from EAS. (b) In the case of $t'_\text{median}/t_\text{median} < 0.5$, we categorize first particle t_1 as coming from a random noise, and the rest as coming from EAS.

tween the OUS1 and the OUS4 (OUS1+4), the data period is from August 2008 to December 2010, and the total observation time is 785 days. The total number of events is about 1.3×10^5 events and 7.3×10^2 events can be estimated those primary energy.

We adopt events determined as $r_{\text{obs}} > 100\text{m}$. Additionally, in order to minimize the contamination of the random noises due to atmospheric muons or thermal noise of the detector, we rejected the events of $t'_\text{median}/t_\text{median} < 0.5$ as shown in Fig. 3, where t'_median is the median value obtained from $t_i - t_2$ ($i = 2, \dots, n - 1$). The noise rate was estimated 0.4% from data.

The coincidence criterion for the time difference between the OUS1 and the OUS4 are within $10\mu\text{s}$ and the time difference distribution is shown in Fig. 4. And we used events within 25.6° in the criterion of EAS zenith angle.

5 Result

Fig. 5-(a) and (b) show the primary energy spectra obtained by the OUS1 and the OUS1+4, respectively. The

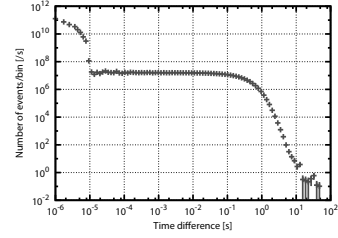


Figure 4: The time different distribution between the OUS1 and the OUS4.

obtained data spectra are fitted by a single power-law spectrum $f'(E)$ and index α' . α' in the OUS1 and the OUS1+4 are equal to -2.46 ± 0.13 and -2.99 ± 0.21 in the primary energy region of $10^{16} - 10^{19.5}\text{eV}$, respectively. Since a true spectrum index α needs to be converted from α' , we obtained α by using the relation between α and α' shown in Fig. 6, and summarized α and α' in Table 1. However, the obtained spectrum shows the index value gradually changes to flattening around 10^{18}eV . Then, we divided the obtained energy spectrum into two region of $10^{16} - 10^{18.5}\text{eV}$ and $10^{18} - 10^{19.5}\text{eV}$, and also fitted in each energy region. Obtained α and α' are shown in Table 1. Note that we could not perform the fitting in the OUS1+4, because there are no events in the energy region above 10^{19}eV . Comparison of the OUS1's α value to the OUS1+4's one in the energy region of $10^{16} - 10^{19.5}\text{eV}$, the energy spectrum of the OUS1+4 is steeper than that of OUS1. The reasons for the difference are that the energy resolution of the OUS1+4 is improved than that of the OUS1 as shown in Fig. 7, and the number of events leaked toward higher energies can be decreased. Accordingly, the OUS1+4 can suppress the flattening of the primary energy spectrum.

Table 1: The spectral index α' and α .

| | | Primary energy region [eV] | | |
|--------|-----------|----------------------------|------------------------|------------------------|
| | | $10^{16} - 10^{19.5}$ | $10^{16} - 10^{18.5}$ | $10^{18} - 10^{19.5}$ |
| OUS1 | α' | -2.46 ± 0.13 | -2.75 ± 0.19 | -2.09 ± 0.08 |
| | α | $-2.54 (+0.22 - 0.24)$ | $-3.20 (+0.52 - 1.3)$ | $-2.09 (+0.17 - 0.03)$ |
| OUS1+4 | α' | -2.99 ± 0.21 | -3.24 ± 0.22 | — |
| | α | $-3.13 (+0.28 - 0.38)$ | $-3.60 (+0.41 - 0.90)$ | — |

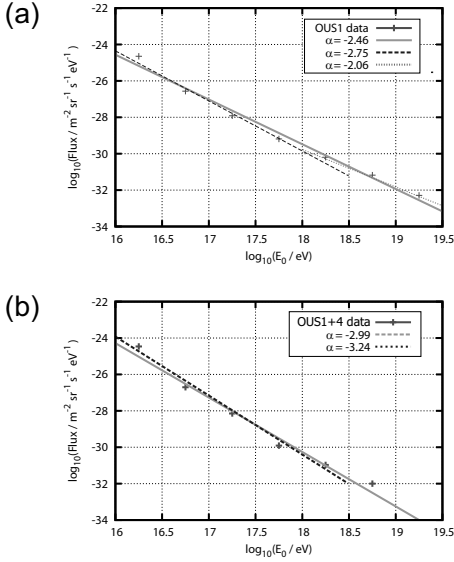
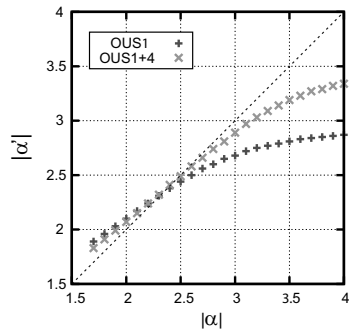


Figure 5: The energy spectra obtained by (a) the OUS1 and (b) the OUS1+4.

Figure 6: The relation α and α' in the OUS1 and the OUS1+4.

6 Conclusion

The primary energy spectrum is obtained by compact EAS arrays and Linsley's method. In the OUS1 observation, true α values are equal to $\alpha = -2.54 (+0.22 - 0.24)$ and $-3.20 (+0.52 - 1.3)$ in the energy region of $10^{16} - 10^{19.5}$ eV and $10^{16} - 10^{18.5}$ eV, respectively. Additionally, in order to improve the energy resolution of the OUS1,

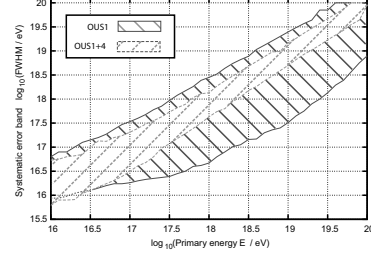


Figure 7: The difference of the energy resolution as function of the primary energy. The hatched band of solid line and dashed line represent the energy resolution in the OUS1 and the OUS1+4.

we have installed the OUS4. In the OUS1+4 observation, α are equal to $\alpha = -3.13 (+0.28 - 0.38)$ and $-3.60 (+0.41 - 0.9)$ in the same region above, respectively. However, the statistics of the OUS1+4 observation data is not enough to discuss the primary energy spectrum above 10^{18} eV, we need more observation time.

References

- [1] F. Schüssler *et. al.*, Proc. 31st ICRC Lodz, 2009
- [2] M. I. Pravdin *et. al.*, Proc. 31st ICRC Lodz, 2009
- [3] K. Shinozaki *et. al.*, Nucl. Phys. B (Proc. Suppl.), 2006, **151**(issue 1): 3-10
- [4] M. Okita *et al.*, Nucl. Phys. B (Proc. Suppl.), 2008, **175-176**, 322-325.
- [5] H. Matsumoto *et. al.*, Nucl. Instr. & Meth. A, 2010, **614**: 475-482
- [6] J. Linsley and L. Scarsi, Phys. Rev., 1962, **128** 2384-2392
- [7] T. Wada *et al.*, Nucl. Phys. B (Proc. Suppl.), 1999, **75**(issue 1-2) 330-332
- [8] N. Ochi *et al.*, J. Phys. G: Nucl. Part. Phys., 2003, **29** 1169-1180
- [9] A. Iyono *et al.*, Nucl. Phys. B (Proc. Suppl.), 2006, **151** 69-72
- [10] J. Linsley, J. Phys. G: Nucl. Phys., 1986 **12** 51-57
- [11] S. J. Sciutto, astro-ph/9911331, 1999
- [12] S. Ostapchenko, Phys. Rev. D, 2006, **74**(issue 1) 014026
- [13] A. M. Hillas, Nucl. Phys. B (Proc. Suppl.), 1997, **52**(issue 1) 29-42